World Academy of Science, Engineering and Technology
International Journal of Materials and Metallurgical Engineering
Vol:5, No:7, 2011

Global and Local Structure of Supported Pd Catalysts

V. Rednic, N. Aldea, P. Marginean, D. Macovei and C. M. Teodorescu, E. Dorolti and F. Matei

***Abstract*—**The supported Pd catalysts were analyzed by X-ray diffraction and X-ray absorption spectroscopy in order to determine their global and local structure. The average particle size of the supported Pd catalysts was determined by X-ray diffraction method. One of the main purposes of the present contribution is to focus on understanding the specific role of the Pd particle size determined by X-ray diffraction and that of the support oxide. Based on X-ray absorption fine structure spectroscopy analysis we consider that the whole local structure of the investigated samples are distorted concerning the atomic number but the distances between atoms are almost the same as for standard Pd sample. Due to the strong modifications of the Pd cluster local structure, the metal-support interface may influence the electronic properties of metal clusters and thus their reactivity for absorption of the reactant molecules.

***Keywords*—**metal-support interaction, supported metal catalysts, synchrotron radiation, X-ray absorption spectroscopy, X-ray diffraction

I. Introduction

THE Palladium nanoparticles were widely investigated since it proved to be very efficient in the hydrogen absorption but also Pd has remarkable properties as a supported metal catalyst.Single-sized palladium clusters have demonstrated enhanced solubility of hydrogen relative to the bulk [1]. In metal-hydrogen alloys, hydrogen absorption occurs by hydrogen atoms occupying interstitial sites, which causes metal atoms to be displaced from their ideal sites as studied by X-ray diffraction (XRD) [2]. Those experiments demonstrated Pd-Pd length expansion in hydrogenated Pd nanoclusters. However, the size effect of hydrogen absorption on the Pd nanocluster lattice has not been studied systematically as a function of the cluster size and structure. For example, in the XRD study [2] the larger clusters were proposed to be cubic, while the smaller ones – icosahedral.On the other hand supported Pd catalysts are widely used today for different catalytic reactions: oxidation of methane, cumene hydroperoxide (CHP) hydrogenation, combustion of hydrocarbons, hydrogenation of propene, ethylene, acetylene and trans-2-pentene, hydrodechlorination, etc [3-8].Particle size effects are a common phenomenon in heterogeneous catalysis. In many cases, such effects are related to the presence of specific reactive sites on particles of particular size and structure or to the modification of geometric or electronic properties as a result of the limited size of the particle or the influence of the support.Extended X-ray absorption fine structure (EXAFS) studies of small palladium particles demonstrate that the activity of hydrogenation catalysts can be clearly linked to the presence or absence of metal-support interaction. Control of this interaction can lead to higher activities for small particles and thus to more efficient catalysts.The aim of this paper is to investigate the global and local structure of the supported Pd catalysts, using the XRD and EXAFS techniques, in order to see the supports influence on the mean crystallites sizes and metal-support interaction.

V. R. Author is with the National Institute for Research and Development of Isotopic and Molecular Technologies, Cluj-Napoca, 400293, Romania (phone: +40264-584.037; fax: +40264-420.042; e-mail: vrednic@itim-cj.ro).

N. A. Author is with the National Institute for Research and Development of Isotopic and Molecular Technologies, Cluj-Napoca, 400293, Romania (e-mail: naldea@itim-cj.ro).

P. M. Author is with the National Institute for Research and Development of Isotopic and Molecular Technologies, Cluj-Napoca, 400293, Romania (e-mail: marginea@oc1.itim-cj.ro).

D. M. Author is with the National Institute of Materials Physics, 077125 Magurele, Romania (e-mail: dmacovei@infim.ro).

C. M. T. Author is with the National Institute of Materials Physics, 077125 Magurele, Romania (e-mail: teodorescu@infim.ro).

E. D. Author is with the Babes-Bolyai University, Faculty of Physics, 400084 Cluj-Napoca, Romania (e-mail: eugen.dorolti@phys.ubbcluj.ro)

F. M. Author is with the Agriculture Sciences and Medicine Veterinary University, Department of Mathematical and Computer Science, Cluj-Napoca, Romania, (e-mail: faldea@usamvcluj.ro).

II. Experimental

A. Samples preparation

Palladium supported catalyst samples were prepared by incipient wetness impregnation method. As supports the Al_2O_3 p.a. Merck (77.6 m^2/g), TiO_2 catalyst support Alfa Aesar (150 m^2/g) and SiO_2 p.a. BDH (312 m^2/g) were used for preparation of the catalyst samples. The supports were dried in an oven, for 12 hour, at 110 ^{0}C, and then were impregnated with a solution of $PdCl_2$ p.a. acidulated with ClH. After impregnation the samples were dried over night, in an oven, at 110^{0}C, and then calcined 2h at 400^{0}C in flowing nitrogen. The samples were reduced 1h in a hydrogen stream, at 300 ^{0}C. The metallic palladium absorbs a large quantity of hydrogen during the reducing process. This hydrogen is very reactive in the presence of oxygen. Therefore the catalyst samples were passivated in flowing nitrogen with low content of oxygen (ca 0.2%). The atomic percentage of Pd, defined by X = [at. Pd/(at. Pd+M)] x 100%, where M represents Al, Ti or Si, is 2%, 1.9% and 1.1% for Pd/Al_2O_3, Pd/TiO_2 and Pd/SiO_2, respectively.

B. Measurement methods

X-ray powder diffraction measurements for the investigated samples were collected using a Bruker D8 Advance diffractometer, in the Bragg-Bretano (BB) geometry, with Ni filtered Cu K_α radiation, λ=1.54178Å, at room temperature. Because the Pd atomic concentration is small the experimental conditions were choose in such way to obtain the best signal to noise ratio: 5 seconds for each step, initial angle 2θ=35°

and the step 0.02.The X-ray absorption spectra of the Pd supported catalysts and a Pd standard sample were carried out in transmission mode at beamline CEMO of the HASYLAB synchrotron-radiation facility (Hamburg, Germany), with the incident radiation analyzed by a Si(111) double-crystal monochromator. The energy in the spectra ranged between 250 eV before the Pd K edge (24350 eV) and 650 eV above. The catalysts and reference samples were prepared as powders diluted in polyethylene and pressed into pellets of suitable thickness.

III. Theoretical Background of EXAFS

The interference between the outgoing and backscattered electron waves has the effect of modulating the X-ray absorption coefficient. The EXAFS function $\chi(k)$ is defined in terms of the atomic absorption coefficient by

$$\chi(k) = \frac{\mu(k) - \mu_0(k)}{\mu_0(k)} \quad (1)$$

where k is the electron wave vector, $\mu(k)$ refers to the absorption by an atom from the material of interest and $\mu_0(k)$ refers to the absorption by an isolate atom in the free state. Theories of EXAFS based on the single scattering approximation of the ejected photoelectron by atoms in immediate vicinity of the absorbing atom give the following expression for $\chi(k)$ [9]:

$$\chi(k) = \sum_j A_j(k) \sin\left[2kr_j + \delta_j(k)\right] \quad (2)$$

where the sum extends over j^{th} coordination shell, r_j is the radial distance from the j^{th} shell and $\delta_j(k)$ is the total phase shift function due to central and neighbors atoms. The total amplitude function $A_j(k)$ is given by:

$$A_j(k) = \left(\frac{N_j}{kr_j}\right) F\left(k, r_j, \pi\right) \exp\left[-2\left(r_j / \lambda_j(k) - k^2\sigma_j^2\right)\right] \quad (3)$$

In this expression N_j is the number of atoms in the j^{th} shell, σ_j is the root means squares deviation of distance about r_j, $F(k,r,\pi)$ is the backscattering amplitude and $\lambda_j(k)$ is the mean free path function for inelastic scattering. The backscattering factor and the phase shift depend on the kind of atom responsible for scattering and its coordination shell [10]. The analysis of EXAFS data for obtaining structural information [N_j, r_j,σ_j, $\lambda(k)$] generally proceeds by employing the Fourier transform. The radial structure function (RSF), Φ is given by:

$$\Phi(r) = \int_{k_{min}}^{k_{max}} k^n \chi(k) \exp(-2ikr)\, dk \quad (4)$$

where k_{min} and k_{max} represent extreme values of the electron wave vector. The EXAFS signal is weighted by k^n ($n=1, 2, 3$) to get the distribution function of atom distances. Due to truncation data effects in the Fourier transform appear spurious peaks and they often interfere with physical features. To avoid this usually is introduced under the integration, for apodization, a window function describes by different Parzen, Kaiser or Hanning filters [11].

The single shell may be isolated by Fourier transform, then using the inverse Fourier transform of the RSF, the $\chi_j(k)$ corresponding to each coordination shell can be obtained:

$$\chi_j(k) = \left(1/k^n\right) \int_{R_{1j}}^{R_{2j}} WF(r)\Phi(r)\exp(2ikr)\, dr \quad (5)$$

The theoretical equation for $\chi_j(k)$ function is given by:

$$\chi_j(k) = A_j(k)\sin\left[2kr_j + \delta_j(k)\right] \quad (6)$$

where the index j refers to the j^{th} coordination shell. The structural parameters for the first coordination shell are determined by fitting the theoretical function χ_j from Eq. (6) to the experimental one χ_j function derived from Eq. (5). In empirical EXAFS calculation, F and δ_j are conveniently parameterized [9] or are determined by theoretical concepts developed by FEFF computing program [12].

IV. Results and Discussion

A. XRD results

XRD line profiles analysis is a versatile nondestructive method that can be used in obtaining nanostructural information. XRD patterns of the investigated samples are shown in Fig. 1.

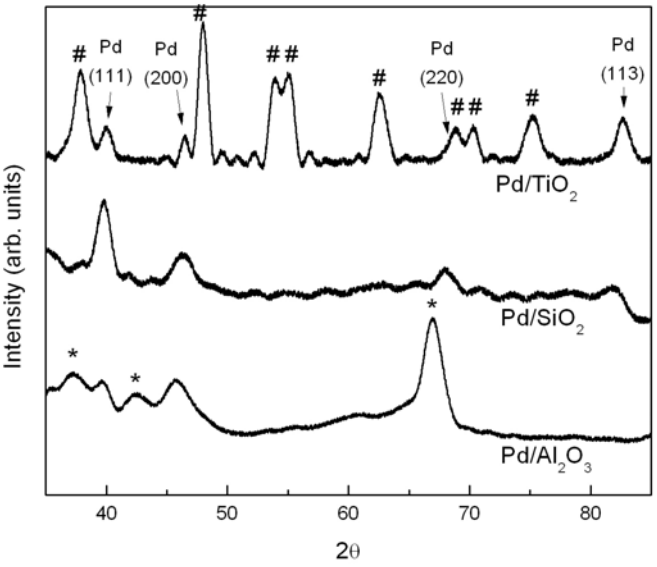

Fig. 1 XRD patterns of the investigated samples. The symbols indicate the XRD peaks associated to the metal oxides supports: #-TiO_2 (anatase) and *-γ Al_2O_3

The peaks corresponding to both the Pd active metal and support oxides were identified, except for SiO_2 which usually presents an amorphous structure.In some regions there is an overlapping between the peaks of Pd and oxides supports. This is why in the processing of XRD patterns were used different Pd XRLPs where such overlapping is not present. The nano-crystallite size is determined by classical Scherrer equation [13]. For a better accuracy in the determination of the full width at half maximum (FWHM), of the XRLP approximation analytical distribution functions like Cauchy, Gauss [14], Voigt [15] or Generalized Fermi Function (GFF)

[16] are used. Goodness of the fit values have shown that the best statistic was obtained for Gauss distribution approximation of the XRLP, like in Fig. 2.

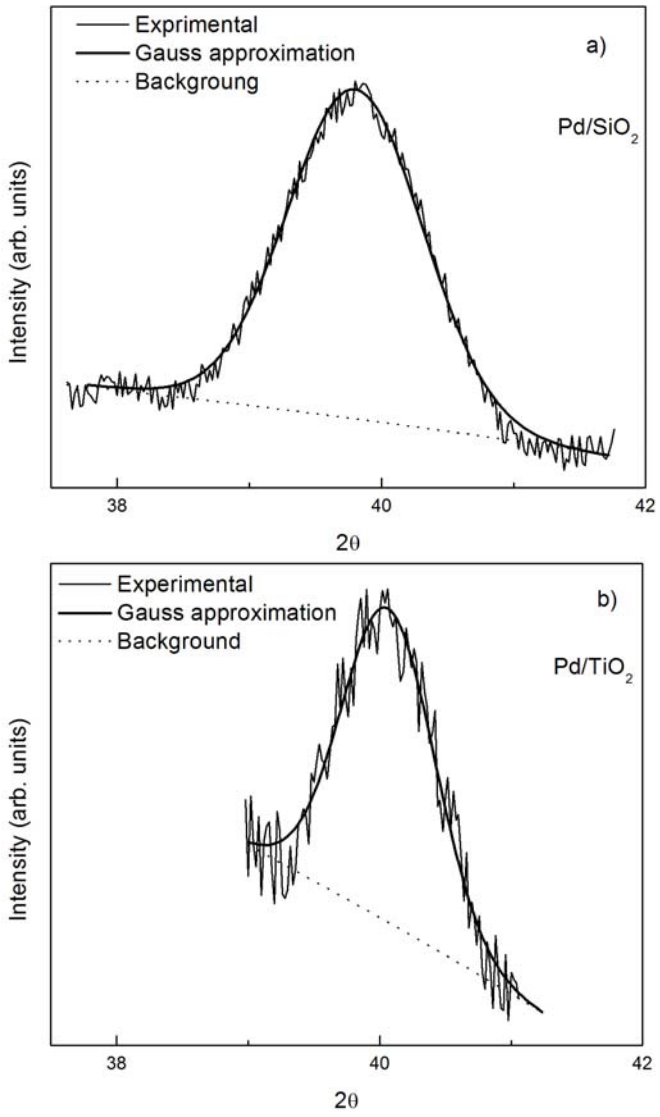

Fig. 2 Pd (111) XRLP of Pt/SiO2 (a) and Pt/TiO2 (b) approximated with an analytical Gauss function type

TABLE I
GLOBAL STRUCTURE PARAMETERS OF THE INVESTIGATED SAMPLES

Sample	hkl	δ_{hkl} [2θ]	FWHM [2θ]	D_{hkl} [Å]
Pd/SiO_2	111	1.2815	1.2039	78
Pd/TiO_2		0.8857	0.8321	113
Pd/Al_2O_3	200	2.1044	1.9769	49

δ_{hkl}- integral width, D_{hkl}-mean diameter of the Pd nanoparticles

Further investigations using Warren and Averbach theory will provide additional information regarding the microstrain parameter and crystallites distribution curve.

B. XAS results

The XAS spectra corresponding to the Pd K were recorded in the energy interval of 24.1-25 KeV. The EXAFS signal is extract based on threshold energy of Pd K edge determination followed by background removal using the well known procedure of the extrapolation of the pre-edge in the post-edge region fitting the base line with polynomial functions. The X-ray absorption coefficient associated to the Pd K edge is shown in Fig. 3 for the investigated samples together with that of Pd standard foil. In this figure E_0 indicates the binding energy position of the Pd K edge determined by the analysis of the first two derivatives of the X-ray absorption near edge structure (XANES).

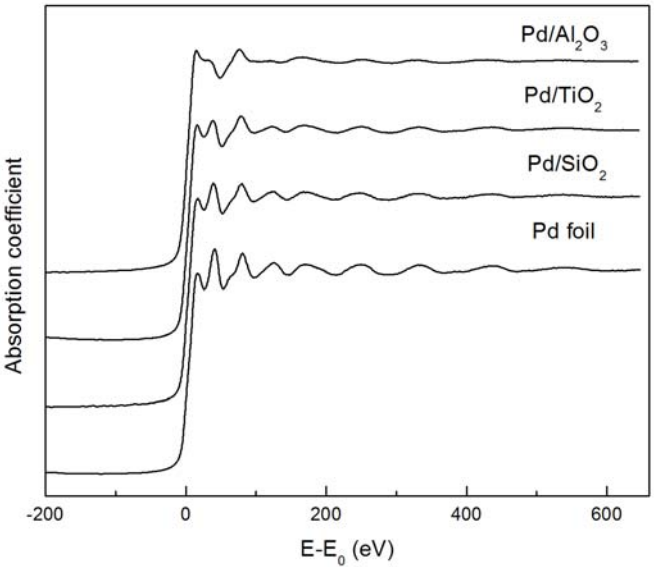

Fig. 3 The normalized absorption coefficients of Pd K edge for investigated samples

The edge position for each investigated sample is given in table 1. It can be seen that there is a difference between the Pd K edge position in supported catalysts and Pd standard sample suggesting an interaction between the Pd and the metal oxide support.Fig. 4 shows the RSF of the Pd/SiO_2 catalyst. Similar results were obtained for the other investigated samples. The Fourier transform peaks are shifted from the true distance due to the phase shift function that is included in the EXAFS signal. In order to avoid spurious errors due to limited interval in the wave vector space we have taken into consideration the Hanning window function, for which the smallest spurious errors were obtained.

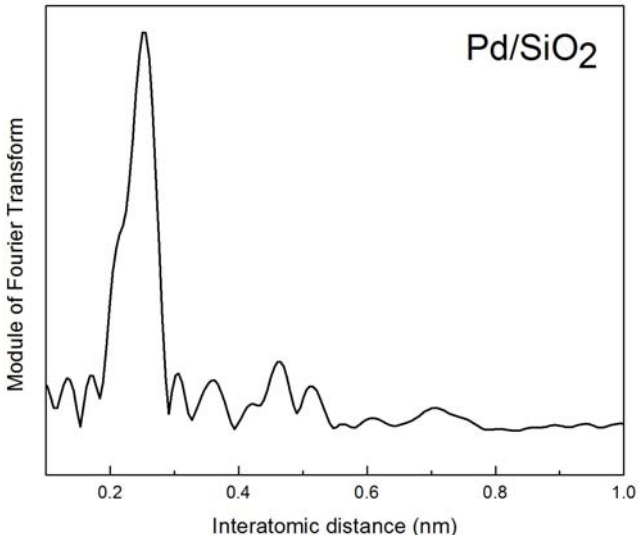

Fig. 4 The Fourier transforms of the EXAFS spectra for Pd supported on SiO_2.

By taking the inverse Fourier transform (IFT) of the first coordination shell contribution we extracted the amplitude envelope function using the ``small perturbation limit'' method [11]. Based on Levenberg-Marquardt fit we evaluated then the interatomic distances, the number of neighbors in the first shell and the edge position. In Fig. 5 the IFT and the simulated spectrum, corresponding to the Pd atoms first coordination shell, for Ni/TiO_2 is given.

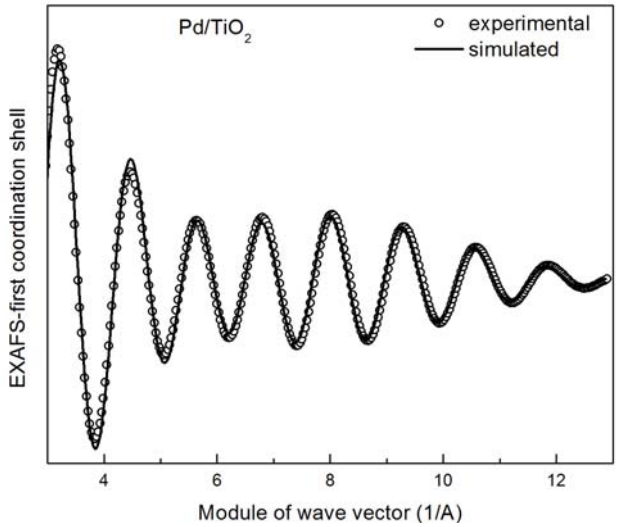

Fig. 5 The experimental and calculated EXAFS signals of the first coordination shell of Pd atoms for Pd supported on TiO_2.

TABLE II
LOCAL STRUCTURE PARAMETERS OF THE INVESTIGATED SAMPLES FOR THE FIRST COORDINATION SHELL

Sample	Coordination number $N_1 \pm \Delta N_1$	Shell radius $R_1 \pm \Delta R_1$ [Å]	Edge position E_0 [eV]
Pd standard	12	3.288	24350
Pd/SiO_2	9.04±0.12	3.291±0.015	24351.55
Pd/TiO_2	6.96±0.11	3.298±0.018	24352.22
Pd/Al_2O_3	6.13±0.13	3.306±0.02	24354.02

On can see that, for the investigated samples compared to the Pd standard sample, there is an important diminution up to 50% in the number of the Pd atoms from the first coordination shell while the average shell radius remains almost constant. We have considered that this diminution of the average nearest-neighbor coordination number is due to a strong electron interaction between the active metal and oxide supports [17-19]. The reduced average nearest Pd-Pd coordination number implies, from the chemical point of view, the existence of the catalytic active centers at the surface of the Pd crystallites.

The Pd nanoparticles supported on Al_2O_3 have the smallest mean size obtained from XRD measurements and presents the maximum deformation of the local structure reflected in the EXAFS measurements. For the other to catalysts there is no correlation between the Pd mean particle size and deformation of the local structure (the number of the Pd atoms in the first coordination shell).

V. Conclusion

XRD measurements have shown that the Pd mean particle size diameter depends on the type of the oxide used as a support; the smallest diameter was obtained when Pd was supported on Al_2O_3.The reduction of the Pd-Pd coordination number from the first coordination shell of the investigated samples points out the existence of the strong electronic interaction between the dispersed Pd nanoparticles and the oxide supports. The deformation of the Pd local structure was more pronounced when it was supported on TiO_2 and Al_2O_3.

Acknowledgment

This work was supported by the research programmers of Romanian Ministry of Education and Research (PN II projects nr. 22098/2008 and 32119/2008). Two of us (DM, CMT) gratefully acknowledge the assistance of Edmund Welter and Dariusz Zajac (HASYLAB) during the EXAFS experiments.

References

[1] C. Sachs, A. Pundt, R. Kirchheim, M. Winter, M. T. Reetz, and D. Fritsch, "Solubility of hydrogen in single-sized palladium clusters", *Phys. Rev. B*, vol. 64, 075408, 2001.

[2] M. Suleiman, N. M. Jisrawi, O. Dankert, M. T. Reetz, C. Bähtz, R. Kirchheim and A. Pundt, "Phase transition and lattice expansion during hydrogen loading of nanometer sized palladium clusters" *J. Alloys and Compounds*, vol. 356-357, pp. 644-648, 2003.

[3] V. Ferrer, D. Finol, D. Rodriguez, F. Dominguez, R. Solano, J. Zarraga and J. Sanchez, "Chemical Characterization and Catalytic Activity of Pd-Supported Catalysts on $Ce_{0.39}Zr_{0.61}O_x/SiO_2$", *Catal Lett*, vol. 132, pp. 292–298, 2009.

[4] Q. Zhu, B. Shen, H. Ling, R. Gu, "Effect of Various Supports on the Catalytic Activity of Pd for Cumene Hydroperoxide Hydrogenation", *Catal Lett*, vol. 132, pp. 464–471, 2009.

[5] Y. Li, Y. Xie and C. Liu, "Enhanced Activity of Bimetallic Pd-Based Catalysts for Methane Combustion", *Catal Lett*, vol. 125, pp. 130–133, 2008.

[6] R. Gopinath, N. S. Babu, J. V. Kumar, N. Lingaiah and P. S. Sai Prasad, "Influence of Pd Precursor and Method of Preparation on Hydrodechlorination Activity of Alumina Supported Palladium Catalysts", *Catal Lett*, vol. 120, pp. 312–319, 2008.

[7] S. Guerrero, P. Araya and Eduardo E. Wolf , "Methane oxidation on Pd supported on high area zirconia catalysts", *Applied Catalysis A: General*, vol. 298, pp. 243-253, 2006.
[8] C. Amorim, G. Yuan, P. M. Patterson and M. A. Keane, "Catalytic hydrodechlorination over Pd supported on amorphous and structured carbon", *Journal of Catalysis*, vol. 234, pp. 268–281, 2005.
[9] N. Aldea, R. Turcu, A. Nan, I. Craciunescu, O. Pana, X. Yaning, Zhonghua Wu, D. Bica, L. Vekas and F. Matei, "Investigation of nanostructured Fe_3O_4 polypyrrole core-shell composites by X-ray absorption spectroscopy and X-ray diffraction using synchrotron radiation", *J.Nanopart. Res.*, vol. 11, pp. 1429-1439, 2009.
[10] E. A. Stern, "Theory of EXAFS" in *X-ray absorption: principles, applications, techniques of EXAFS, SEXAFS and XANES*, D.C. Koningsberger, R. Prins, Ed. New York: Weley, 1988.
[11] A. San-Miguel, "A program for fast classic or dispersive XAS data analysis in a PC", *Physica B.*, vol. 208&209, pp. 177-179, 1995.
[12] J. J. Rehr, J. Mustre de Leon, S. I. Zabinsky, R. C. Albers, "Theoretical x-ray absorption fine structure standards", *J. Am. Chem. Soc.*, vol. 113, no. 14, pp. 5135–5140, 1991.
[13] B. E. Warren, "Diffraction by imperfect crystals" in *X-Ray Diffraction*, Ed. New York: Dover Publication, pp. 251-254, 1990.
[14] H.P. Klug and L.E. Alexander, "X-Ray Diffraction Procedures for Polycrystalline and Amorphous Materials", 2nd ed., Ed. New York: John Wiley and Sons, 1974, pp. 618-708.
[15] D. Balzar, "X Ray Diffraction Line Broadening: Modelling and Applications to High –Tc Superconductors", *J. Res. Nat. Inst. Stand. Technol.*, vol. 98, pp. 321-353, 1993.
[16] N. Aldea, A. Gluhoi, P. Marginean, C. Cosma and X. Yaning, "Extended X-ray absorption fine structure and X-ray diffraction studies on supported nickel catalysts", *Spectrochim. Acta B*, vol. 55, pp. 997-1008, 2000.
[17] D. C. Koningsberger and B. C. Gates, "Nature of the metal-support interface in supported metal catalysts: results from X-ray absorption spectroscopy", *Catal. Lett.*, vol. 14, pp. 271-277, 1992.
[18] C. H. Lin, S. H. Hsu, M.Y. Lee and S. D. Lin, "Active morphology of Au/γ-Al_2O_3-a model by EXAFS", *J. Catal.*, vol. 209, pp. 62-68, 2002.
[19] R. Zanella, S. Giorgio, C. H. Shin, C. R. Henry, and C. Louis, "Characterization and reactivity in CO oxidation of gold nanoparticles supported on TiO2 prepared by deposition-precipitation with NaOH and urea", *J. Catal.*, vol. 222, pp. 357-367, 2004.